Syst. Biol. 61(4):595–607, 2012

DOI:10.1093/sysbio/sys002
Advance Access publication on January 4, 2012

The Evolution of Defense Mechanisms Correlate with the Explosive Diversification of Autodigesting *Coprinellus* Mushrooms (Agaricales, Fungi)

LÁSZLÓ G. NAGY[1,*], JUDIT HÁZI[1], BALÁZS SZAPPANOS[2], SÁNDOR KOCSUBÉ[1], BALÁZS BÁLINT[3], GÁBOR RÁKHELY[4], CSABA VÁGVÖLGYI[1], AND TAMÁS PAPP[1]

[1]*Department of Microbiology, Faculty of Science and Informatics, University of Szeged, Kozep fasor 52., H-6726 Szeged, Hungary;* [2]*Institute of Biochemistry, Biological Research Centre, Hungarian Academy of Sciences, Temesvári krt. 62., H-6726 Szeged, Hungary;* [3]*Cancer Epigenetics and Biology Program (PEBC), The Bellvitge Institute for Biomedical Research (IDIBELL), Hospital Duran i Reynals, Av. Gran Via de L'Hospitalet 199-203, 08907—L'Hospitalet de Llobregat, Barcelona, Spain; and* [4]*Department of Biotechnology, Faculty of Science and Informatics, University of Szeged, Kozep fasor 52., H-6726 Szeged, Hungary;*
**Correspondence to be sent to: Department of Microbiology, Faculty of Science and Informatics, University of Szeged, Kozep fasor 52., H-6726 Szeged, Hungary; E-mail: cortinarius2000@yahoo.co.uk.*

Received 11 March 2011; reviews returned 23 May 2011; accepted 3 October 2011
Associate Editor: Mark Fishbein

Abstract.—Bursts of diversification are known to have contributed significantly to the extant morphological and species diversity, but evidence for many of the theoretical predictions about adaptive radiations have remained contentious. Despite their tremendous diversity, patterns of evolutionary diversification and the contribution of explosive episodes in fungi are largely unknown. Here, using the genus *Coprinellus* (Psathyrellaceae, Agaricales) as a model, we report the first explosive fungal radiation and infer that the onset of the radiation correlates with a change from a multilayered to a much simpler defense structure on the fruiting bodies. We hypothesize that this change constitutes a key innovation, probably relaxing constraints on diversification imposed by nutritional investment into the development of protective tissues of fruiting bodies. Fossil calibration suggests that *Coprinellus* mushrooms radiated during the Miocene coinciding with global radiation of large grazing mammals following expansion of dry open grasslands. In addition to diversification rate–based methods, we test the hard polytomy hypothesis, by analyzing the resolvability of internal nodes of the backbone of the putative radiation using Reversible-Jump MCMC. We discuss potential applications and pitfalls of this approach as well as how biologically meaningful polytomies can be distinguished from alignment shortcomings. Our data provide insights into the nature of adaptive radiations in general by revealing a deceleration of morphological diversification through time. The dynamics of morphological diversification was approximated by obtaining the temporal distribution of state changes in discrete traits along the trees and comparing it with the tempo of lineage accumulation. We found that the number of state changes correlate with the number of lineages, even in parts of the tree with short internal branches, and peaks around the onset of the explosive radiation followed by a slowdown, most likely because of the decrease in available niches. [Autodigestion; diversification; fungi; hard polytomy; key innovation; speciational model; stochastic character mapping; veil.]

Episodes of accelerated speciation are believed to have produced much of Earth's extant diversity. Classic examples of explosive diversification are found among plants (Richardson et al. 2001; Klak et al. 2004; Egan and Crandall 2008; Valente et al. 2010) and animals (Verheyen et al. 2003; Joyce et al. 2005; Kozak et al. 2006; Rundell and Price 2009), but no examples are known among fungi or microbes, most probably because of the lack of a continuous fossil record and comprehensive phylogenies. Advanced phylogenetic methods now permit the investigation of the tempo and mode of diversification in the absence of a continuous well-documented fossil evidence. With the fungal genus *Coprinellus* (Psathyrellaceae, Agaricomycetes) as a model, in this paper, we report on explosive speciation in fungi for the first time and examine various aspects of the accumulation of morphological diversity within this radiation. *Coprinellus* is a monophyletic group of fungi with spectacular autodigesting fruiting bodies, which produce chitinolytic enzymes to digest themselves into a blackish fluid and are used as models in developmental biology (Lim and Choi 2009). *Coprinellus* comprises one of four lineages in the Psathyrellaceae with autodigesting fruiting bodies and we have recently demonstrated that switches between nonautodigesting and autodigesting fruiting bodies represent a distinguished period of evolution, referred to as coprinoidization (Nagy et al. 2010; Nagy et al. 2011). Coprinoidization entails a series of morphological and physiological changes that accelerate the ontogeny of the fruiting bodies. It has been hypothesized that the fast ontogeny enables these mushrooms to colonize substrates with considerably fluctuating water content. However, patterns of the diversification of autodigesting lineages and their fit in the environment are still poorly understood.

The theory of adaptive radiations predicts a relationship between the rates of phenotypic and species diversification (Schluter 2000; Purvis 2004), but evidence for this has remained marginal due to the small number of carefully studied examples and the scarcity of suitable morphological data sets (Pagel 1999a, 2006; Harmon et al. 2003; Purvis 2004; Ricklefs 2004; Adams et al. 2009; Agrawal et al. 2009; Organ et al. 2009; Lanfear et al. 2011). Because adaptive radiations are characterized by rapid partitioning of the available niches and the phenotype space, a correlation between morphological and species diversification can be viewed as phylogenetic evidence for an adaptive radiation as compared with nonadaptive radiations (Kozak et al. 2006; Rundell and Price 2009). Furthermore, a high rate of trait evolution

early in the radiation, followed by a deceleration, has been suggested as rapidly radiating species fill available niches (Schluter 2000; Kozak et al. 2006; Agrawal et al. 2009), but experimental evidence for this is scarce, and its generality throughout the tree of life remains to be established. Recently developed models and theoretical considerations imply association between trait evolution and species diversification, but few studies have demonstrated its existence (Hunter and Jernvall 1995; Hunter 1998; de Queiroz 2002; Donoghue 2005), even fewer have shown causality (Hodges and Arnold 1995). Such key innovation hypotheses predict that certain intrinsic evolutionary innovations boost diversification by opening new niches to the organisms or increase their fitness (Sanderson and Donoghue 1994; Hodges and Arnold 1995; Hunter 1998). Despite their perplexing morphological diversity, key innovation hypotheses have not been proposed for fungi so far. Within *Coprinellus*, previous taxonomic classifications took advantage of various characteristics of the veil, a protective layer on the cap and stipe surfaces, the size and color of the fruiting bodies, size and shape of the spores, the presence, absence, and shape of specialized hairs on the cap surface and habitat. It is noteworthy that, within the Psathyrellaceae, hairs occur exclusively in *Coprinellus* and that the proportion of coprophilous species is also the highest there. Despite elaborate taxonomic knowledge of these groups, the evolution of, and thus the potential effect on diversification, the abovementioned traits are not known. Therefore, in this study, we attempt to single out those that may be associated with species diversification.

In this paper, we examine the temporal dynamics of the diversification of the Psathyrellaceae with emphasis on morphological traits. We use multigene data sets of the Psathyrellaceae and *Coprinellus* (this latter nearly complete at the species level) to make inferences about the tempo of species accumulation and perform ancestral character state reconstructions to find morphological traits that explain differences in diversification between clades.

Materials and Methods

Taxon Sampling, Generation of Sequence Data, and Alignment

To design taxon sampling for phylogeny reconstruction, we collected taxonomic information relating to species of Psathyrellaceae, with special emphasis on *Coprinellus*, from two major sources: literature searches and taxonomic identification and examination of herbarium specimens. Species for inclusion in phylogenetic analyses were selected to ensure maximum taxonomic coverage in all clades of the family, while, at the same time maintaining the proportions of true diversity in each clade. To mitigate further the bias originating from cases of inhomogeneous species concepts, we relied on two critical monographs in the case of European species for *Coprinopsis*, *Coprinellus*, and *Parasola* (Uljé and Bas 1991) and for *Psathyrella* (Örstadius 2008) and revised specimens and original descriptions of North American and tropical species. Specimens for this study were obtained from public herbaria (WU, MICH, NY, AH, K, L, KR, WTU, SzMC, and E) and from moist chamber experiments (i.e., incubating soil, wood, and dung samples at high humidity for 3 weeks and harvesting fruiting bodies; see Doveri et al. 2010). Detailed studies of all coprinoid specimens were undertaken in three herbaria (Herbarium of the University of Leiden, L; Burke Museum of Natural History and Culture, WTU; Herbarium of the Department of Microbiology, University of Szeged, SzMC), which together comprise the three largest collections of these fungi worldwide (totaling ca. 5000 specimens).

Genomic DNA was purified from 10 mg of dried material by means of the DNeasy Plant Mini Kit (Qiagen). PCR amplification targeted four nuclear loci, the nuclear ribosomal large subunit (LSU, 1.5 kb), the ITS1-5.8S-ITS2 (0.8 kb) regions and portions of the elongation factor 1α (ef−1α, 1.2 kb), and β-tubulin (0.5 kb) genes. PCR conditions, primer use, and sequencing are described in Nagy et al. (2011). Ambiguous bases were coded as "N".

We supplemented new sequence data with sequences from previously published phylogenies (Larsson and Orstadius 2008; Padamsee et al. 2008; Vasutova et al. 2008; Nagy et al. 2009; Nagy et al. 2010; Nagy et al. 2011) (online Table 1, available from Dryad data repository; doi: 10.5061/dryad.665vv1c7). Alignment of sequences was computed by ClustalW (Thompson et al. 2002) for the LSU, ef−1α, and β-tubulin genes followed by manual adjustments, whereas ITS sequences have been aligned by Probalign (Roshan and Livesay 2006).

Interlocus phylogenetic conflict was tested by the approximately unbiased test as implemented in CONSEL (Shimodaira and Hasewaga 2001; Shimodaira 2002). For each alignment, maximum likelihood (ML) trees were estimated in 10 replicates and per-site likelihood values were computed in RaxML 7.0.1 (Stamatakis 2006). These were imported into CONSEL, which was launched with default parameters. AU-test P values < 0.06 were interpreted as an evidence of significant conflict.

Data Sets and Model Selection

Two data sets were assembled for this study, one spanning the whole Psathyrellaceae and a subset of this focusing on *Coprinellus*; the former was used to test diversification rate variation and the latter to investigate the build-up of morphological diversity, ancestral state reconstructions, and polytomy analyses. The larger data set includes all 13 major clades of Psathyrellaceae (Hopple and Vilgalys 1999; Keirle et al. 2004; Walther et al. 2005; Larsson and Orstadius 2008; Padamsee et al. 2008; Vasutova et al. 2008; Nagy et al. 2009; Nagy et al. 2010; Nagy et al. 2011). One specimen per species was included in both data sets. Representatives of the closely related Bolbitiaceae (*Bolbitius vitellinus*, *Conocybe lactea*, *Agrocybe pediades*, *A. praecox*, and *Mythicomyces corneipes*)

were used to root the family level phylogeny. The *P. candolleana* clade was inferred sister to *Coprinellus*; thus, we used *P. candolleana*, *P. badiophylla*, and *P. leucotephra* as outgroups for the smaller data set.

We selected nucleic acid models for the data sets using the AIC_c criterion, as implemented in jModeltest (Posada 2008). During model selection, the proportion of invariant sites (I) was not considered, since this basically accounts for the same phenomenon as the gamma distribution, and unidentifiability problems have been reported when the two parameters are applied simultaneously for the same data set in Bayesian MCMC frameworks (Rannala 2002; Stamatakis 2006). As best-fit models, jModeltest selected the GTR + G model for the ITS1, ITS2, nrLSU, ef−1α, and β-tubulin gene regions, whereas for the 5.8S gene, the JC69 model was suggested. The partitioning regime used in all phylogenetic analyses have been adopted from our previous work, in which several alternative partitioned models have been compared on the basis of Bayes Factors (Nagy et al. 2011). Thus, for all analyses, data were partitioned into ITS1 (1–905), 5.8S (906–1082), ITS2 (1083–1889), nrLSU (1890–3189), ef−1α (3190–3852), and β-tubulin (3853–4228) regions, and the evolutionary model was estimated for each partition separately.

Phylogenetic Analyses

Analyses of the 69-taxon data set.—Phylograms for the smaller data set were inferred in MrBayes and BayesPhylogenies (Pagel and Meade 2007a) to compare the topologies and posterior probabilities across the two programs and models. We ran the Markov chains for 30,000,000 generations, sampling every 1000th generation. In BayesPhylogenies, we inferred trees under mixture models, which represent a generalization of the GTR + G model to include intrapartition heterogeneities in evolutionary patterns (Pagel and Meade 2005), by estimating 4 GTR + G matrices for each partition in our case. MrBayes was launched with four incrementally heated chains and two simultaneous replicates, whereas in BayesPhylogenies, three replicates with only one chain per replicate were run. A burn-in with wide safety margins was established as 15,000,000 generations by checking the convergence of likelihoods in Tracer 1.4 (Rambaut and Drummond 2008b) and topological convergence by using AWTY (Wilgenbusch et al. 2004). The resulting 15,000 trees were used to compute 50% Majority Rule phylograms from the output of each program. Posterior probabilities higher than 0.94 were considered significant.

We also inferred trees for this data set under the assumption of a molecular clock in BEAST 1.6.1 (Rambaut and Drummond 2008a). We used an uncorrelated lognormal relaxed molecular clock model and the partitioning regime outlined above. The tree prior was set to the Yule process. Twenty-five million generations were run, and the sampling frequency was set to every 1000th generation. Thus, we sampled 25,000 trees, of which the first 15,000 were discarded as burn-in. BEAST analyses were run in three replicates. TreeAnnotator was used to find the Maximum Clade Credibility tree. The output of this analysis was used to construct lineages through time (LTT) plots (see below).

The 242-taxon data set.—We inferred phylograms for this data set by using MrBayes 3.1.2. Data partitioning, models, and chain length for this analysis were as above for the smaller alignment, but the sampling frequency was set to 100 and an ML empirical prior for branch lengths was invoked. This latter aimed to mitigate systematic overestimation of branch length reported for MrBayes, which can result in unrealistic branch lengths and inflation of Bayesian posterior probabilities for long trees (Brown et al. 2010; Marshall 2010). We formalized the parameter of the exponential prior on branch lengths as $\lambda = -\ln(0.5)/\Psi$, where Ψ is the mean of the branch lengths taken from a ML tree.

Like the smaller data set, the 242-taxon alignment was analyzed under an uncorrelated lognormal relaxed molecular clock model in BEAST. To avoid potential effects of prior choice on the estimation of diversification rates, we ran identical analyses under both tree priors implemented in BEAST: the Yule model and the Birth–Death model. Chain length, sampling, and burn-in were as above. All other parameters were left at their default values. Chronograms were calibrated with dates from our previous study, in which several indirect and fossil and composite calibrations outside the Psathyrellaceae were compared (Nagy et al. 2010). We defined a normal prior distribution for the genera *Parasola*, *Coprinellus*, and *Coprinopsis* with a mean and standard deviation chosen to include the range of credible values obtained by six calibration schemes (Nagy et al. 2011), excluding the extreme estimates yielded by the Heckman et al. (2001) calibration (see Nagy et al. 2011, p. 311). Thus, we set mean/standard deviation of 50/20, 95/30, and 80/25 for the most recent common ancestors of *Coprinellus*, *Coprinopsis*, and *Parasola*, respectively.

Polytomy Analyses

Explosive radiations are usually characterized by explosive, if not simultaneous accumulation of lineages. In such cases, the relationships of the resulting species are best described by a star phylogeny, also called a hard polytomy, whereas bifurcating trees represent a poor description of the evolutionary history. Although expansive polytomies constitute the key signature of explosive diversification (Valente et al. 2010), it is difficult to reject the null hypothesis that the polytomy is caused by an inadequate or insufficient sample of characters. Therefore, we propose a new framework for examining adaptive radiations by analyzing the resolvability of internal nodes via Bayesian analysis. For this, we employed Phycas 1.2.0 (Lewis et al. 2010), a Bayesian MCMC package, to estimate the posterior probabilities of internal nodes of *Coprinellus* being polytomies. To visit incompletely resolved trees, besides traditional

Larget-Simon moves, the MCMC proposal mechanism in Phycas uses "add-edge" and "delete-edge" moves, which allow jumps between trees of different resolution. This reversible-jump MCMC method, when run long enough, directly measures the posterior probability of a node being resolvable.

We examined the effects of various prior distributions on the results by applying two qualitatively different prior distributions, "resolution class" and "polytomy" priors. Within both categories, four "prior strength" values ($\delta = 0.5$, $\delta = 1.0$, $\delta = e$ and $\delta = e^2$) corresponding to the informativeness of the prior were tested (Fig. 1, online Fig. 3). With a prior strength of δ, a topology or a resolution class has δ times the probability compared with a more or a less resolved topology or resolution class, respectively. A resolution class is defined as the universe of trees with the same number of polytomic nodes (Lewis et al. 2010). Thus, $\delta = 0.5$ represents a "polytomy unfriendly" prior, $\delta = 1.0$ is a flat prior, whereas $\delta > 1.0$ puts higher prior probability on less resolved trees. Of the flat priors, a resolution class prior is a completely uninformative distribution with regard to the resolvability of nodes, whereas the polytomy prior is not, since it puts equal probability on each topology, and there are many more incompletely resolved topologies than fully resolved ones. To examine prior impact further, we ran analyses on each gene and the combined alignment separately and with sampling from the prior only, resulting in 64 MCMC runs in total. The ef−1α gene was omitted from these analyses, since it was available for <50% of setulose *Coprinellus* species. We partitioned the data as above and ran 100,000 cycles (1 cycle equals ca. 200 "traditional" Bayesian generations [Lewis et al. 2010]) in the trials of prior impact and single-gene analyses and 200,000 cycles in the final analyses of the combined data set. The topology prior for the final analyses was an uninformative resolution class prior ($\delta = 1.0$). Every 10th cycle was sampled. Burn-in was set to 50,000 and 100,000 cycles for the single-gene and final analyses, respectively.

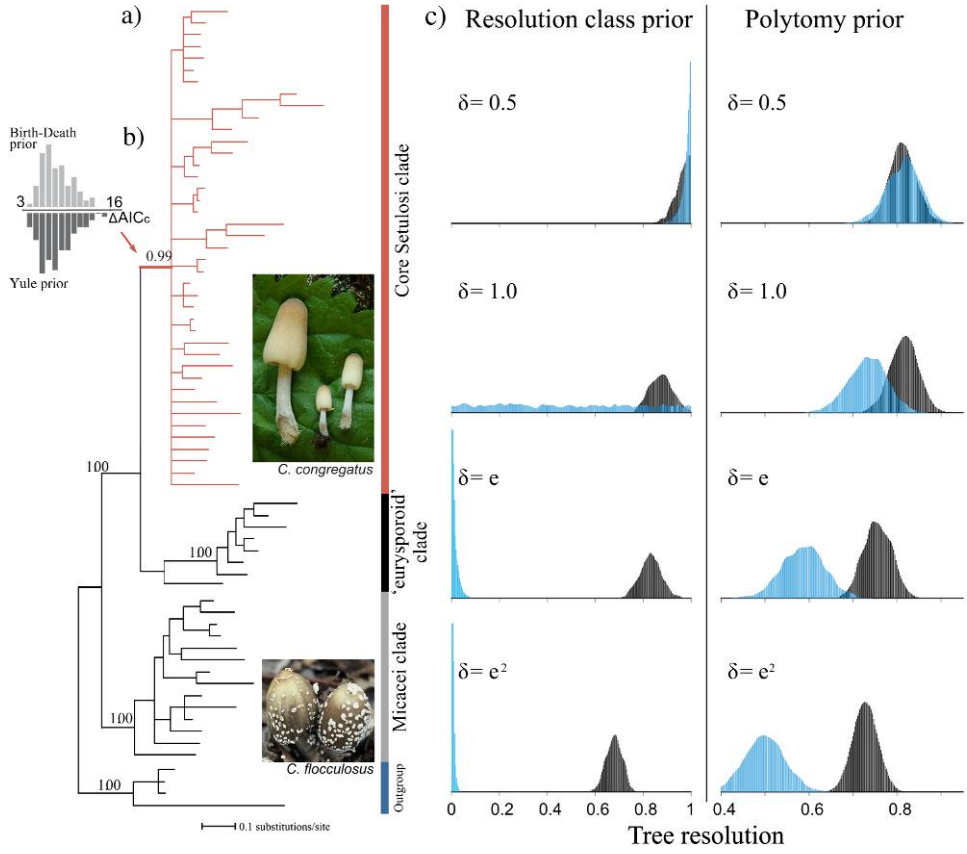

FIGURE 1. Explosive radiation of the Core Setulosi clade. a) Analysis of the resolvability of internal nodes of *Coprinellus* revealed an expansive polytomy at the backbone of the Core Setulosi clade, whereas resolution of the sister clades is high. This is consistent with the hard polytomy hypothesis that should be observable when species radiate into available niches at a high rate, (nearly) simultaneously. The tree is a 50% Majority Rule consensus of 10,000 phylograms inferred from the concatenated four-gene alignment (4228 sites) by using Reversible-Jump MCMC. The analysis was run under an uninformative resolution class polytomy prior, which assigns equal probability to each class of tree resolution. The arrow shows the shift in diversification rate. b) The distribution of MEDUSA ΔAIC_c values under two tree priors. Numbers above selected branches denote Bayesian posterior probabilities. c) Prior and posterior distributions of tree resolution in the polytomy analyses of the four-gene data set as inferred under resolution class and polytomy priors and four prior-strength values (δ). Skewness of posterior distributions (black) toward values around 0.75–0.8, as compared with priors (blue; gray in print version), reveal a strong phylogenetic signal in the data outweighing that of the prior.

Analyses of Diversification

LTT plots were constructed for the Core Setulosi clade and the Micacei clade, using the R package APE (Paradis et al. 2004). We drew a sample of 1000 + 1000 chronograms from the 2 replicates of the BEAST analyses and pruned the trees to contain species of the Core Setulosi and Micacei clades only. Net rates of diversification (speciation – extinction) were calculated for clades comprising more than 10 taxa according to Nee (2001) in the Laser R package (Rabosky 2006). For these analyses, we used the 242 taxon data set and sampled 1000 ultrametric phylogenies in BEAST assuming both the Yule and BD processes.

We applied the Measuring Evolutionary Diversification Using Stepwise AIC (MEDUSA) framework to find shifts in diversification rates in the presence of taxonomic information for each of the clades (Alfaro et al. 2009). Briefly, the method estimates rates of the Birth–Death model and stepwisely adds breakpoints to the phylogeny, stopping the procedure when the likelihood of the resulting n-breakpoint model is not significantly better than that of the model with $n - 1$ sets of rates (specified by the AIC_c cutoff value). We performed MEDUSA analyses by using the R library Geiger (Harmon et al. 2008) on a sample of 50 + 50 chronograms under the Yule and BD tree priors. To avoid effects of sparse sampling in the outgroup, we removed the outgroup taxa and retained *M. corneipes* only. We examined the robustness of our results to the MEDUSA analysis parameters "cutAtStem", "modelLimit", and "estimateExtinction". We compiled species richness data from the most recent monographic treatments of the genera *Coprinopsis*, *Coprinellus*, *Parasola*, and *Psathyrella* (for details, see online information) and our revisions of herbarium type and voucher specimens. The taxonomic study of Psathyrellaceae species is fortunately immune to substantial differences in species concepts, with few notable exceptions (as opposed to other species-rich fungal groups, e.g., *Cortinarius*, *Inocybe*, *Russula*, etc.). Based on morphological similarity, 62 unsampled species were assigned a relationship and formalized as a richness table used in the MEDUSA analyses. Even with this depth of sampling, it is likely that some species remained uninvolved, but their distribution is certainly random, so they introduce no bias in our analyses.

Analyses of Morphological Evolution

We inferred the temporal distribution of character state changes along the phylogeny by using 42 taxonomically informative morphological/ecological traits (for a list and description, see online Figs. 4 and 5). To obtain a Bayesian sample of state changes, we used stochastic character mapping by drawing n "mutational maps", consistent with the ancestral states and the prior distribution on rates. The mutational maps provide information about the duration of a state along a particular branch, which can be used to calculate the total distance of the state changes from the tips/root. Under Markovian models, longer branches are expected to give more opportunity to a character to change, which renders molecular branch length information in explosive radiations (with many short internal branches) misleading. Thus, what is desired is a method that uses only the information in the terminals of the tree, which we accomplished by using a tree with each branch of unit length (Agrawal et al. 2009). We employed SIMMAP 1.5.1 (Bollback 2006) to draw 1000 mutational maps from the posterior distribution for each of the 100 post-burn-in trees and morphological/ecological traits. Optimization of priors followed Ekman et al. (2008), by counting the average number of state changes for each character under parsimony (in MacClade 4.08) and defining a gamma distribution with a mean at the inferred number of state changes. The gamma distribution was discretized using 60 rate categories, and the total tree length was rescaled to 1.0 in all cases. We then calculated the distance of the state changes from the root and from the terminals using the original branch lengths of the trees. Thus, bias arising from the short internal branches during the rapid diversification could be overcome (Cunningham 1999). Subsequently, we divided the timescale to 1000 discrete bins, counted the number of state changes in each, and normalized with the number of lineages present in each bin. We repeated the analyses both with samples of chronograms and phylograms under binary and multistate coding of traits (see online information). A perl package for performing the above analyses is available from the authors.

Morphological Model Inferences and Ancestral State Reconstructions

We took an empirical Bayesian approach to infer models and reconstruct ancestral states for traits, which show a characteristic distribution within the Core Setulosi and Micacei clades and based on superficial inspection of ancestral state reconstructions in SIMMAP may correlate with shifts in diversification rates. In this manner, the presence of hairs and a macroscopically discernable veil have been identified as candidates. Both were modeled by continuous time Markov models in BayesTraits 1.0 (Pagel and Meade 2007b) under speciational and gradual modes of evolution. To select best-fit models, we first estimated rates by ML on 100 phylogenies under gradual and speciational modes of evolution. We then compared models implying no gains ($q_{01} = 0$), no losses ($q_{10} = 0$), and equal rates of gain and loss (Nagy et al. 2010) (Table 2) and chose the one with the fewest parameters not rejected against the free model by the LRT-like statistic for nonnested models (Pagel and Meade 2007b).

Ancestral state reconstructions were performed on the gradual and speciational trees for four clades: the genus *Coprinellus*, Micacei clade, Core Setulosi clade, and All-Setulosi clade (eurysporoid clade + Core-Setulosi). Nodes were defined by the "mrca" command,

and ancestral states were estimated by ML for each tree in the sample. A fully Bayesian method was also considered, but with regard to the dependence of posterior distributions on the prior and the difficulties in finding reliable priors, we took ML instead. Both model inferences and ancestral state reconstructions were performed on a sample of 1000 phylograms of the 69-taxon data set obtained from MrBayes.

RESULTS

Data Sets

As a result of revisions of herbarium specimens, we included 69 species in the smaller data set (taxon sampling 88%), whereas the larger one comprised 242 species with a taxon sampling density > 70% in most clades (except for three small groups, the *Cystoagaricus*, *Psathyrella calcarea*, and *P. cotonea* clades; Table 1), which probably constitutes the most comprehensive family-level agaric phylogeny to date. The data set includes several unnamed species, mainly in the genera *Parasola*, *Coprinopsis*, and *Coprinellus* but also in psathyrelloid clades. A detailed taxonomic treatment of these species is in preparation for submission to a mycological journal or has been published elsewhere (Nagy 2006; Doveri et al. 2010; Házi et al. 2011) (online Fig. 6).

After the exclusion of ambiguously aligned regions, both concatenated alignments comprised 4228 sites of nucleic acid. The approximately unbiased test did not indicate significant conflict among the data sets. Almost all the species were represented by at least two genes (mostly ITS and LSU), 172 by three regions, and 91 by all four gene regions. PCR amplifications of two or more loci from *C. singularis*, *C. simulans*, *C. parvulus*, and *C. ephemerus* failed. This latter turned out to be rarer than previously assumed, whereas the closely related *C. congregatus* is very common. Comparison with formerly published phylogenies revealed that the missing data did not influence the recovery and support values of larger clades, since the gross topology of the tree is congruent with that obtained for the species represented by all four genes and a 126-taxon tree with a much smaller proportion of missing data (Nagy et al. 2010; Nagy et al. 2011). All newly generated sequences have been deposited in GenBank (online Table 1).

TABLE 1. Taxon sampling density in Psathyrellaceae clades

Clades	Percentage of species included in the phylogeny reconstruction (%)
Coprinopsis	77
Core *Setulosi* clade	85
Coprinellus p.p. 1	82
Cystoagaricus clade	54
eurysporoid clade	100
Lacrymaria clade	88
Parasola	88
Psathyrella calcarea clade	60
Psathyrella candolleana clade	80
Psathyrella cotonea clade	50
Psathyrella fusca clade	82
Psathyrella gracilis clade	73
Psathyrella senex clade	100[a]
Psathyrella spadiceogriseae clade	75

Note: Clade diversities were compiled from literature and revisions of herbarium specimens.
[a]This clade may contain some additional species, for which it is difficult to establish clear affinities.

Phylogenetic Analyses

Trees inferred for the 242-taxon data set in BEAST and MrBayes were congruent, differing only in the placement of the Lacrymaria clade, a basal relationship which proved difficult to resolve (Larsson and Orstadius 2008; Padamsee et al. 2008; Nagy et al. 2010; Nagy et al. 2011). In all analyses, *Coprinellus* was split into three strongly supported clades, which we denote as Core Setulosi, eurysporoid, and Micacei clades (Fig. 1, online Figs. 1 and 2), corresponding to the morphologically established sections *Setulosi*, *Setulosi* p.p., and *Micacei* + *Domestici*, respectively (Uljé 2005). Within *Coprinellus*, the position of *C. sabulicola* was somewhat uncertain, appearing either as a sister species to the eurysporoid clade or basal to the eurysporoid + Core Setulosi clade.

Polytomy Analyses

Reversible-Jump MCMC runs converged quickly to the stationary distributions as judged from the convergence of likelihoods and split posterior probabilities. Under all 32 prior settings (8 different priors on 4 data sets each), the majority of the sampled trees had one or more polytomies. With uninformative polytomy priors, which assign equal probability to each distinct tree topology, including resolved and unresolved ones, the mean resolution varied between 0.8 [95% highest posterior density (HPD): 0.7–0.89] for β-tubulin, 0.73 (95% HPD: 0.64–0.82) for nrLSU, 0.77 (95% HPD: 0.70–0.84) for ITS, and 0.87 (95% HPD: 0.82–0.93) for the concatenated data set, which together correspond to 5–22 unresolved nodes per tree. The resolution of the 50% Majority Rule consensus trees was much lower, with the highest resolution achieved in the combined analysis (0.56, 30 unresolved nodes). Uninformative resolution class priors are much more conservative, though, the mean resolution of sampled trees is highly consistent with those obtained under polytomy priors: 0.58 (95% HPD: 0.43–0.76) for β-tubulin, 0.71 (95% HPD: 0.62–0.80) for nrLSU, 0.76 (95% HPD: 0.64–0.84) for ITS, and 0.87 (95% HPD: 0.78–0.97) for the concatenated data set (online Fig. 3). Comparison of MCMC sampling of trees with and without data reveals a strong signal in our data with regard to the resolvability of internal nodes. Although there was a positive correlation between mean resolution of the sampled topologies and increasing alignment length, even with all three genes combined, the Markov Chains spent >99% of their time at unresolved topologies under a uniform prior and >80% when a prior favoring fully resolved trees was assumed. Polytomies were inferred most frequently for

the basal nodes of the Core Setulosi clade, whereas relationships within both the eurysporoid and the Micacei clade were almost fully resolved on the 50% consensus phylograms (Fig. 1a).

Diversification Analyses

By fitting models of diversification with zero, one or more shifts in diversification rates to an ultrametric 242-taxon phylogeny of the Psathyrellaceae (by using the MEDUSA framework [Alfaro et al. 2009]), we found that the phylogeny is best described by a birth–death model in which the tempo of diversification increases on the branch leading to the Core Setulosi clade (Fig. 1, online Figs. 1 and 2). The AIC_c values did not differ significantly across the tree samples obtained under the Yule and BD speciation priors in BEAST (ΔAIC_c = 3.02 – 15.69). Models with multiple diversification rate shifts yielded significantly worse likelihood values on all trees. The rate shift has been located on the branch leading to the Core Setulosi clade. Varying the parameters "CutAtStem", and "EstimateExtinction" did not have considerable effect on the results.

Net rates of diversification (speciation minus extinction) have been calculated for all clades with more than 10 taxa for a Bayesian sample of chronograms and are presented as Figure 2. The highest mean rate was inferred for the Core Setulosi clade (0.032 lineages/myr). Thus, diversification in the Psathyrellaceae has been slow, with an abrupt speedup between the Eocene to the Miocene (≈38 Ma, 95% HPD: 58.7–18.3 Ma) in the most recent common ancestor of the Core Setulosi clade. LTT plots recover a greater slowdown for the Micacei clade as compared with the Core Setulosi clade (Fig. 3). Furthermore, the slope of the curves implies a higher diversification rate in the Core Setulosi clade than in the Micacei clade, which accords well with our estimates of net rates of diversification (Fig. 3).

Morphological Diversification

We estimated the temporal distribution of character state changes on the 69-taxon data set for all taxonomically informative morphological and ecological traits by using SIMMAP. On average, the stochastic mapping analyses resulted in $7 - 9 \times 10^7$ state changes per tree sample and the results were consistent across trait coding regimes (binary/multistate) and tree samples (chronograms/phylograms). We obtained the distribution of state changes by calculating for each of the path length from the tip or the root of the tree for chronograms or phylograms, respectively. We then divided the timescale of chronograms into 1000 bins and calculated the number of state changes that fall into each of the bins. The resulting distribution (Fig. 3) was used as a proxy for the speed of morphological diversification. All alignments, trees, and morphological data sets have been deposited in TreeBASE (Study No. 11138).

The results of model comparisons and ancestral state reconstructions for veil and hairs using BayesTraits under gradual and speciational modes of evolution were congruent. For the veil, a model implying no gains within *Coprinellus* have been suggested as the best, whereas the model with no losses of veil yielded the worst likelihood values. A model implying the opposite pattern was found to fit best the evolution of veil, whereas models with no gain and equal rates were significantly rejected. Ancestral state reconstructions suggest veiled, hair-less ancestors for the Micacei clade and the genus *Coprinellus* and veil-less, haired ancestors for the Core Setulosi clade and 'All-Setulosi' clade (Core Setulosi + eurysporoid). The ancestral habitat type in the Core Setulosi clade is ambiguous (Table 3), and there is discordance between the results obtained under gradual and speciational models, whereas ancestors of the other three examined clades were reconstructed as non-coprophilous. Furthermore, unlike veil and hairs, no model could be singled out as significantly better than

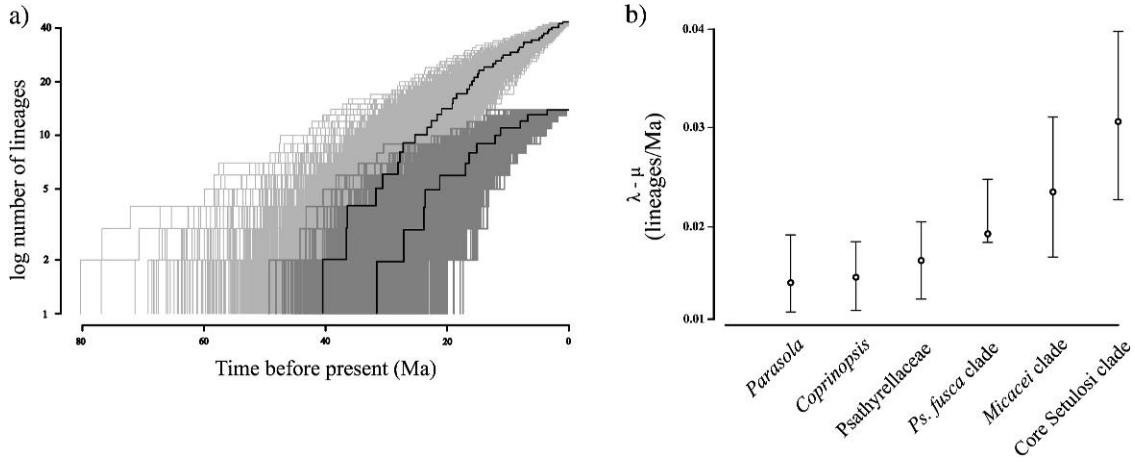

FIGURE 2. The temporal dynamics of the radiation. a) LTT plots showing very modest or no slowdown in the rate of diversification for the Core Setulosi clade (light gray) as compared with the Micacei clade (dark gray). Numbers of lineages are shown on a log scale. b) Net rates of diversification (speciation minus extinction) in clades of the Psathyrellaceae with >10 taxa. Both LTT plots and the estimation of speciation and extinction rates are based on 1000 post-burn-in trees sampled after stationarity under an uncorrelated lognormal molecular clock model.

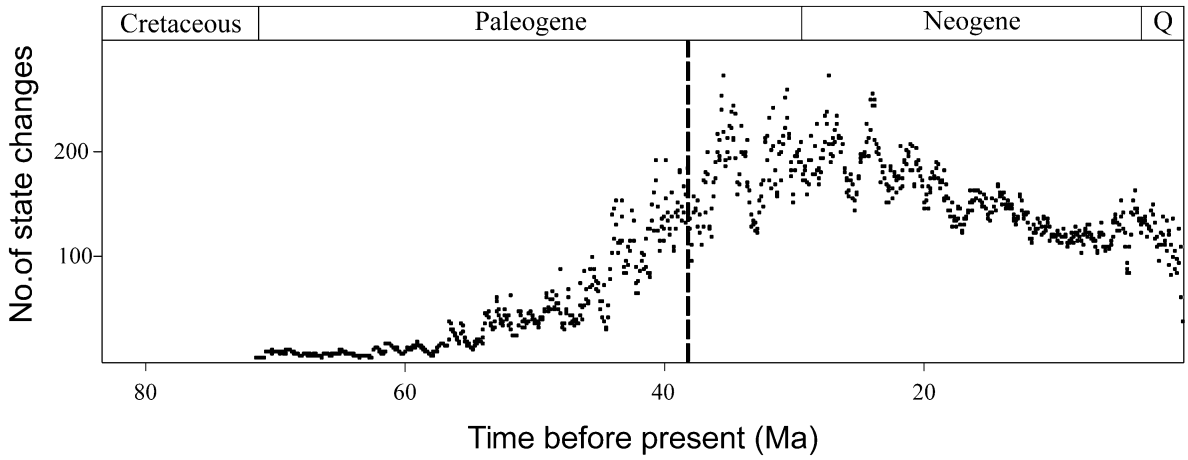

FIGURE 3. Deceleration of morphological diversification in the Core Setulosi clade. The diagram shows the relative frequency of state changes in 37 binary morphological traits as inferred by stochastic mapping and normalized with the number of branches in each of the 1000 discrete bins the timescale was divided to. One-thousand mappings were performed on each of 100 post-burn-in speciational trees, and the distance of the state changes from the tips was traced back by using the original branch lengths of the (ultrametric) trees. The same results were obtained for an alternative trait coding regime (42 characters in total) and for phylograms. The "y" axis denoted the number of state changes per lineage per tree sample. The long left tail is caused by uncertainty in the tree sample. Dashed line shows the mean age of the Core Setulosi clade (38.4 Ma). "Q" stands for Quaternary.

others, except for the one in which gains of coprophyly are impossible, which was significantly worse than others ($2\,(\ln L_1 - \ln L_0) = 12.39$ and 7.02 under gradual and speciational models, respectively).

DISCUSSION

Polytomy Analyses

To test whether species emerged (nearly) simultaneously, we employed a Bayesian sampler that uses Reversible-Jump MCMC (Lewis et al. 2005, 2010) to visit both resolved and unresolved topologies. In the Reversible-Jump MCMC framework, the frequency of trees in the posterior distribution that include a polytomy at the node of interest can be used to estimate the posterior probability of that node being a hard polytomy, given the data set used. Traditional Bayesian approaches have been shown to become unpredictable and tend to place high posterior probability on any arbitrary resolution around the polytomous node in case one tries to resolve a node that exists as a hard polytomy in nature (Lewis et al. 2005). In real biological examples, such settings can occur when the tree contains "branches" along which no or very few substitutions have occurred, as expected in (neutrally evolving) loci when either the speciation rate is high or the rate of molecular evolution is too low to reconstruct the branch properly.

If used to examine explosive radiations, distinguishing methodical artifacts from biologically meaningful polytomies can be challenging. Such artifacts involve the conflict between data partitions and insufficient length of alignments, as well as incongruence in tree samples as a result of poor topological convergence, all of which can produce a high proportion of polytomous nodes on the phylogeny. Low resolution caused by conflicting tree signal between alignments (e.g., because of introgression, incomplete lineage sorting, or reticulate evolution) can be accounted for by using traditional combinability tests (Shimodaira 2002), whereas the contribution of alignment length to the lack of resolution is more difficult to assess objectively. Previous attempts to test the hard polytomy hypothesis were based on the statistical comparison of polytomous and resolved trees (Fishbein et al. 2001) or the presence of phylogenetic signal along paths between species of the putative radiation at various distances from each other (Jackman et al. 1999). Sister clades to the putative radiation can provide a clue for that since they can be regarded as internal controls when their resolvability is compared with that of the clade of the putative radiation, given that taxon sampling and the rate of molecular evolution are approximately the same in both. In our example, the resolution of the Micacei and eurysporoid clades contrast significantly with that of the Core Setulosi clade, suggesting that the expansive polytomy in the latter is not a result of the brevity of the concatenated alignment, given that the distribution of the phylogenetic signal in the alignment is uniform across the tree. As a counterexample, in single-gene analyses, we observed the loss of resolution for all three clades simultaneously when only β-tubulin was analyzed (online Fig. 3). In this case, the lack of resolution could most likely be attributed to the weakness of the phylogenetic signal in the data set, (the β-tubulin alignment was only 375-bp long). In this case, the extent to which the shape of posterior distributions differ from that of priors can provide a clue for the strength of the signal in the data. This is particularly problematic when early evolutionary events are being scrutinized, such as class- or phylum-level phylogenies. It has been proposed that the resolution of such early divergences may require a tremendous number of

alignment sites, which even phylogenomic studies may fail to produce (Fishbein et al. 2001; James et al. 2006; Hackett et al. 2008; Struck et al. 2011). In a previous example, parametric bootstrapping suggested that unrealistically long alignments ($>10^7$ sites) may be required to resolve basal relationships in the Saxifragales, an example of multifurcating speciation (Fishbein et al. 2001). Polytomy analyses might prove particularly useful for resolving old explosive radiations, where methods using estimates of speciation and extinction rates fail due to problems in taxon sampling and the detection of extinct lineages. In general, polytomy analyses can complement the shortcomings of currently routinely applied diversification rate–based methods for detecting explosive radiations. Since polytomy analyses do not require the estimation of speciation and extinction rates, they are expected to be less prone to bias in taxon sampling and tree imbalance. The nonoverlapping assumptions of polytomy analyses and diversification rate–based methods described above enable a more comprehensive examination of putative explosive radiations.

During our analyses of *Coprinellus*, the Markov chains spent on average >99% of their time at unresolved trees. Although priors on tree topology had a considerable effect on the posterior distribution of tree resolvability, the shape of the posterior was dominated by the phylogenetic signal from the data, and comparison of the different prior-posterior pairs revealed an unambiguous pattern about node resolvability (Figs. 1 and 2). When uninformative priors on tree topology were enforced, the number of unresolved nodes per single-gene tree varied between 5 and 22 (mean tree resolution: 0.64 – 0.93), centered on the backbone of the Core Setulosi clade (Fig. 1), suggesting that it constitutes a hard polytomy and conforms to a period of rapid diversification early in the evolution of this clade. Another explanation for the lack of resolution may be the conflicting phylogenetic signal in the data or inadequate length of the alignment. Both can be excluded in our case, since no conflict was detected between the genes and the length of the concatenated alignment (4228 sites) is comparable to some of the most elaborate species-level data sets.

Evolution of Morphological Traits

The theory of adaptive radiations predicts that the build up of morphological diversity should be rapid early in the radiation, possibly followed by a deceleration as the availability of niches limits diversification (Schluter 2000; Kozak et al. 2006; Rabosky and Lovette 2008). It recently became possible to study such processes for continuously varying traits in a phylogenetic framework (Pagel 1999b; Freckleton and Harvey 2006; Agrawal et al. 2009). Here, we present a framework for discrete traits that is analogous to observing the overall morphological diversity within a clade at successive time intervals, a philosophy similar to that of LTT plots. Normalization of the number of state changes by the number of lineages in each successive time interval outlines a figure of the speed and temporal dynamics of morphological diversification by using discrete traits. One potential limitation of this approach is that numerous characters are needed to reliably estimate the dynamics of diversification, an aspect requiring further study.

Model-based inferences of phenotypic evolution along phylogenetic trees have a great potential, especially for poorly fossilizing organisms and/or traits. However, modeling the effects of speciation/extinction on phenotypic evolution and vice versa has a number of assumptions that may or may not be met under some evolutionary processes. One of the most important questions may be whether and when the rate of molecular evolution can be extrapolated to the rate of phenotypic evolution and, thus, whether molecular branch length (even if estimated accurately) represents a good approximation of the number of state changes in phenotypic traits. Phylogenetic inference from putative neutrally evolving loci fails to capture the amount and nature of evolutionary events along a branch of a tree when either the tempo of speciation or phenotypic evolution differ from that of molecular evolution considerably. Adaptive radiations are typical such cases, when the use of molecular branch length for comparative studies of nonmolecular characters (morphological, behavioral, etc.) cannot be justified (Cunningham 1999). By disregarding branch length information (in the speciational model), our analysis used only the distribution of character states in the terminals and the number of internal nodes to infer the placement and number of character transitions along a phylogenetic path. The "chance" for inferring adaptive radiation with such settings is higher than with molecular branch lengths, however, the use of molecular branch lengths would introduce a much bigger bias in model-based analyses by repulsing state changes from the short internal branches of the radiation. In this respect, our approach is similar to parsimony mapping except that it allows multiple substitutions to occur along a particular branch. Whether a molecular branch length model, a speciational model in which the branch lengths correspond to the number of speciation events (Agrawal et al. 2009) are set equal length (present study), or a model in which branch lengths for each character are transformed by a ML optimized scaling factor (κ or λ, [Pagel 1994, 1997]) would yield the least biased test of adaptive radiation using discrete traits requires further theoretical and empirical study. Models not assuming a constant rate of trait evolution across the phylogeny (Skinner 2010) may provide an alternative to laboring with branch lengths, although the dependency of the estimation of transition probabilities on branch lengths and the difficulty of keeping the number of parameters and the variance of the estimate low would not be eliminated.

We found that the accumulation of morphological diversity correlates with that of lineages, even in parts of the tree with short internal branches, suggesting an elevated rate of morphological diversification early in Core Setulosi clade followed by a deceleration (Fig. 4). The number of state changes peaks around the onset of

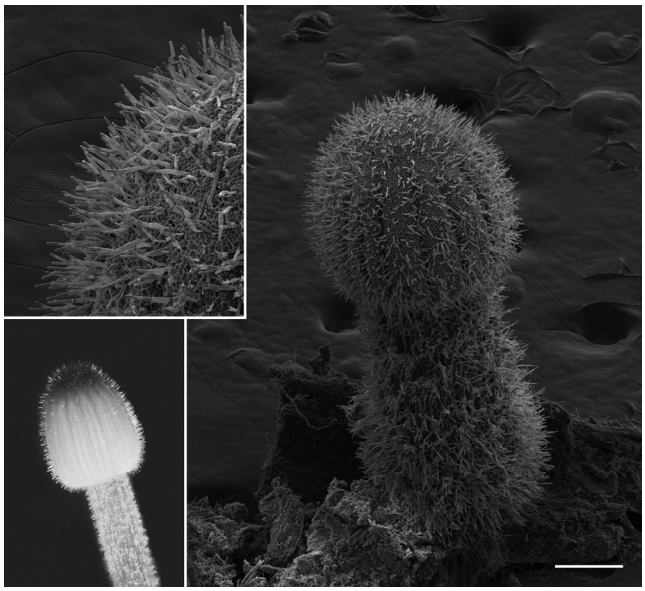

FIGURE 4. Hairs on the cap surface of *Coprinellus pellucidus*. Hairs evolve by elongation of the apical region of cap cells (visible as the background of hair coverage), whereas veil structures of other *Coprinellus* species is composed of many layers of spherical cells that differentiate from the underlying cap tissues. The scale bar is 200 μm for the right image.

the radiation, suggesting a "rapid-early" morphological diversification for the Core Setulosi clade. This observation underpins one of the central theoretical predictions of adaptive radiations, that is, a high rate of trait change early in the history of the clade followed by a slowdown as the number of available niches decrease (Schluter 2000; Purvis 2004; Agrawal et al. 2009).

Are There Morphological Traits Correlated with Diversification?

The Core Setulosi clade shares many life history traits with the rest of the family, such as autodigestive fruiting bodies, habitat preferences, and geographic distribution. Therefore, ecological or dispersal events alone cannot explain the observed differences in diversity. Key innovation hypotheses have been proposed as an explanation of changes in speciation rates in response to the emergence of traits relaxing certain constraints on diversification. Therefore, we looked for traits that show a correlation with the shift in diversification rate. One of the most spectacular traits that may affect the diversification capacity of *Coprinellus* species are velar structures (online Fig. 4/p-s), which cover the young fruiting bodies of several fungal groups and display substantial morphological diversity in the Psathyrellaceae. Velar structures are widespread and conserved in Agaricomycete fungi and take several forms, including volvae or patches of *Amanita* species and ring or collar-like structures. All veil structures serve to protect immature fruiting bodies and spore-bearing surfaces and are known in the majority of agaric families. Hairs (also called pilocystidia, specialized elongate cells of the cap tissue, Fig. 4, online Fig. 4) represent another type of cap covering structure found only in *Coprinellus*, where the Core Setulosi clade contains >90% of haired species. Ancestral state reconstructions show that there is a reciprocal relationship between the presence of veil and hairs, that is, the veil in *Coprinellus* species with hairs is reduced or absent (Table 2). Both structures serve to protect fruiting bodies from mycophagous insects and/or moisture. Comparisons of unidirectional models of trait evolution with bidirectional, equal rates, and unequal rates models suggest that evolving hairs is the preferred way for *Coprinellus* species (Tables 2 and 3), whereas the best-fit model for the veil implies that gains are impossible and that veil coverage has been lost in *Coprinellus* ($2\,(\ln L_1 - \ln L_0) = 4.87 - 18.62$). Branches along which reduction of the veil may have taken place are close to or identical to those which gave rise to hairs (Table 3), suggesting that hairs took over the defense function of velar structures. During the ontogeny of the mushroom, development of hairs via elongation of the apical part of the cap cells does not require differentiation of highly specific layers of the cap as the veil does (Reijnders

TABLE 2. Comparison of models of traits evolution for putative key innovations under speciational and gradual modes of evolution

	Presence of macroscopically visible veil (lnL)	Habitat coprophilous (lnL)	Presence of hairs on the cap surface (lnL)
Speciational (k) mode			
Unconstrained model	−78,619	−275, 307	−133, 669
Constrained model $q_{01} = q_{10}$	−99, 054	−278, 032	−16, 278[a]
Constrained model $q_{01} = 0$	**−78,619**	−337, 254[a]	−170, 747[a]
Constrained model $q_{10} = 0$	−171, 726[a]	−276, 284	**−133,668**
Gradual mode			
Unconstrained model	−80, 288	−267, 523	−134, 071
Constrained model $q_{01} = q_{10}$	−112, 152[a]	−273, 625	−170, 205[a]
Constrained model $q_{01} = 0$	**−80,288**	−302, 614[a]	−175, 645[a]
Constrained model $q_{10} = 0$	−177, 481[a]	−271, 186	**−134,071**

Notes: The likelihoods reported are means of lnL values obtained for 100 phylogenies. The models containing the fewest parameters not rejected by the hypothesis test [$2(\ln L_1 - \ln L_0) < 2.00$, where L_1 is the unconstrained model and L_0 is the alternative, constrained model] are shown in bold.

[a]Denotes that the model yields significantly worse [$2(\ln L_1 - \ln L_0) \geqslant 2.00$] likelihood values than the unconstrained model. q_{01} stands for the rate of gain of veil, coprophyly and hairs, q_{10} stands for rates of loss.

TABLE 3. Ancestral state reconstructions of the presence of veil and hairs as well as coprophilous habitat at deep nodes of *Coprinellus*

Trait/clade	Gradual mode	Speciational mode
Presence of macroscopically visible veil		
Core Setulosi clade	**0.9996**	**0.9999**
All-Setulosi clade	**0.9877**	**0.9888**
Coprinellus	**0.000**	**0.000**
Micacei clade	**0.000**	**0.000**
Presence of hairs on the cap surface		
Core Setulosi clade	**0.0035**	**0.0036**
All-Setulosi clade	**0.0805**	**0.0808**
Coprinellus	**1.000**	**1.000**
Micacei clade	**1.000**	**1.000**
Habitat coprophilous		
Core Setulosi clade	0.5865	**0.9174**
All-Setulosi clade	**0.6615**	**0.9588**
Coprinellus	**0.7197**	**0.9746**
Micacei clade	**0.803**	**0.9714**

Notes: Probabilities are given for state "0" in all cases, showing the reciprocal relationship between the evolution of veil and hairs. Reconstructions are shown in bold when the likelihood obtained with the node fixed in one of the states was significantly worse than that of the opposite state as judged by the hypothesis test $2(\ln L_1 - \ln L_0) < 2.00$, where L_1 and L_0 are the likelihood of the reconstruction when the node was fixed in state 1 (presence of trait) and state 0 (absence of trait).

1979). Although the biochemical and genomic background of veil and hair development are not known, based on the cellular mechanisms their reciprocal relationship may be regarded as a reduced investment in defense traits, similar to that reported for *Asclepias* (Agrawal et al. 2009). In that case, the loss of the veil and the gain of hairs might have contributed to the explosive radiation of the Core Setulosi clade by relaxing constraints on diversification in *Coprinellus* through decreasing the nutritional investment in defense traits. Other, unexamined characters may also correlate with diversification, among others the size of fruiting bodies, but this remains to be tested in a framework for continuous characters. Furthermore, given the difficulty of proving a causative role of the evolution of veil and hairs in the diversification of *Coprinellus*, the presence of such a correlation between veil loss and diversification in other agaric families may provide a further indirect evidence for veil imposing limits on diversification in certain groups. Whether other agarics with reduced or no veil have experienced similar episodes of evolution, what type of alternative defense mechanisms may substitute veil in addition to hairs or how the presence of veil affects the evolution of fruiting bodies in agarics remain to be explored.

Interestingly, the proportion of species (about 50%) inhabiting excrements of extant ungulates and ruminants is much higher in the Core Setulosi clade than in other clades of the Psathyrellaceae. Model comparisons and ASR-s suggest that coprophyly evolved independently in the Core Setulosi and the Micacei clades (10–11 based on parsimony mapping), and the ancestor of the Core Setulosi clade could not be reconstructed unambiguously. Thus, it is likely that frequent habitat shifts characterized the early evolution of this clade, suggesting that these species have been more successful in radiating into the great wealth of niches provided by early herbivorous mammals than taxa of other clades of *Coprinellus*. Large herbivores became the dominant grazers during the Miocene, following significant expansion of grasslands (Janis et al. 2000), which greatly overlaps with the age of the most recent common ancestor of the Core Setulosi clade (59 – 18 Ma). These observations open the way for an exciting ecological hypothesis, that the expansion of open grasslands enabled the radiation of large herbivores, which then created new niches for coprophilous mushrooms.

Whether the loss of veil and/or the emergence of hairs represent key innovations, however, remains an intriguing question, due to the difficulties in establishing causality between character evolution and species diversification. However, if morphological innovations indeed affected diversification, it can acutely bias our conclusions drawn about the trends of the morphological characters involved because the higher abundance of a given state in the clade in which that state promotes diversification would be interpreted as a trend toward that state, when model of independent evolution were used (Maddison et al. 2007).

CONCLUSIONS

Taken together, our study reports the first explosive radiation known in fungi, which shows correlation with a transition to a new defense mechanism. Interestingly, the preferred habitat type and age of the radiating species suggest that the global expansion of grasslands and ungulates have played an important role in this radiation. Very little is known about the large-scale patterns of fungal diversification, but this study raised the possibility that fungal radiations can presuppose the radiation of their substrate or host, which may be even more spectacular in radiations of pathogenic or mycorrhizal fungi. Furthermore, because most fungi are nutritionally dependent on other organisms (saprotrophs, mycorrhizal or pathogenic, probably with the exception of lichens), their spores can disperse over long distances,

and to our best knowledge, their distribution is rarely as structured as that of plants and animals, thus are rarely endemisms and—according to the dominant view—speciate mainly sympatrically (Giraud et al. 2008), it follows that explosive fungal radiations are less likely to fill geographically isolated habitats (such as islands) but more often dependent on the evolution of other organisms and/or intrinsic evolutionary innovations.

Supplementary Material

Supplementary material, including data files and/or online-only appendices, can be found in the Dryad data repository (doi:10.5061/dryad.665vv1c7).

Funding

This work was supported by the Fungal Research Trust (to L.G.N.) and the Hungarian Research Fund (NN75255 to T.P.).

Acknowledgments

We thank Luke Harmon for providing R code for the diversification analyses, Leif Örstadius, Jan Cervenka, Derek Schafer, Tommy Knuttson for loaning materials, and Paul O. Lewis, Gábor M. Kovács and Zsolt Pénzes for discussions on polytomy analyses.

References

Adams D.C., Berns C.M., Kozak K.H., Wiens J.J. 2009. Are rates of species diversification correlated with rates of morphological evolution? Proc. Biol. Sci. 276:2729–2738.

Agrawal A.A., Fishbein M., Halitschke R., Hastings A.P., Rabosky D.L., Rasmann S. 2009. Evidence for adaptive radiation from a phylogenetic study of plant defenses. Proc. Natl Acad. Sci. U.S.A. 106:18067–18072.

Alfaro M.E., Santini F., Brock C., Alamillo H., Dornburg A., Rabosky D.L., Carnevale G., Harmon L.J. 2009. Nine exceptional radiations plus high turnover explain species diversity in jawed vertebrates. Proc. Natl Acad. Sci. U.S.A. 106:13410–13414.

Bollback J.P. 2006. SIMMAP: stochastic character mapping of discrete traits on phylogenies. BMC Bioinformatics 7:88.

Brown J.M., Hedtke S.M., Lemmon A.R., Lemmon E.M. 2010. When trees grow too long: investigating the causes of highly inaccurate Bayesian branch-length estimates. Syst. Biol. 59:145–161.

Cunningham C.W. 1999. Some limitations of ancestral character-state reconstruction when testing evolutionary hypotheses. Syst. Biol. 48:665–674.

de Queiroz K. 2002. Contingent predictability in evolution: key traits and diversification. Syst. Biol. 51:917–929.

Donoghue M.J. 2005. Key innovations, convergence, and success: macroevolutionary lessons from plant phylogeny. Paleobiology 31:77–93.

Doveri F., Sarrocco S., Pecchia S., Forti M., Vannacci G. 2010. Coprinellus mitrinodulisporus, a new species from chamois dung. Mycotaxon 114:351–360.

Egan A.N., Crandall K.A. 2008. Divergence and diversification in North American Psoraleeae (Fabaceae) due to climate change. BMC Biol. 6:55.

Ekman S., Andersen H.L., Wedin M. 2008. The limitations of ancestral state reconstruction and the evolution of the ascus in the Lecanorales (lichenized Ascomycota). Syst. Biol. 57:141–156.

Freckleton R.P., Harvey P.H. 2006. Detecting non-brownian trait evolution in adaptive radiations. PLoS Biol. 4:e373.

Fishbein M., Hibsch-Jetter K., Soltis D.E., Hufford L 2001. Phylogeny of the Saxifragales (Angiosperms, Eudicots): an example of rapid, ancient radiation. Syst. Biol. 50:817–847.

Giraud T., Refrégier G., Le Gac M., de Vienne D.M., Hood M.E. 2008. Speciation in fungi. Fungal Genet. Biol. 45:791–802.

Hackett S.J., Kimball R.T., Reddy S., Bowie R.C., Braun E.L., Braun M.J., Chojnowski J.L., Cox W.A., Han K.L., Harshman J., Huddleston C.J., Marks B.D., Miglia K.J., Moore W.S., Sheldon F.H., Steadman D.W., Witt C.C., Yuri T. 2008. A phylogenomic study of birds reveals their evolutionary history. Science 320:1763–1768.

Harmon L.J., Schulte J.A. 2nd, Larson A., Losos J.B. 2003. Tempo and mode of evolutionary radiation in iguanian lizards. Science 301:961–964.

Harmon L.J., Weir J.T., Brock C.D., Glor R.E., Challenger W. 2008. GEIGER: investigating evolutionary radiations. Bioinformatics 24:129–131.

Házi J., Nagy G.L., Vagvolgyi C., Papp T. 2011. Coprinellus radicellus, a new species northern distribution. Mycol. Prog. 10:363–371.

Heckman D.S., Geiser D.M., Eidell B.R., Stauffer R.L., Kardos N.L., Hedges S.B. 2001. Molecular evidence for the early colonization of land by fungi and plants. Science 293:1129–1133.

Hodges S.A., Arnold M.L. 1995. Spurring plant diversification: are floral nectar spurs a key innovation? Proc. Biol. Sci. 262:343–348.

Hopple J.S. Jr., Vilgalys R. 1999. Phylogenetic relationships in the mushroom genus Coprinus and dark-spored allies based on sequence data from the nuclear gene coding for the large ribosomal subunit RNA: divergent domains, outgroups, and monophyly. Mol. Phylogenet. Evol. 13:1–19.

Hunter J.P. 1998. Key innovations and the ecology of macroevolution. Trends Ecol. Evol. 13:31–36.

Hunter J.P., Jernvall J. 1995. The hypocone as a key innovation in mammalian evolution. Proc. Natl Acad. Sci. U.S.A. 92:10718–10722.

Jackman T.R., Larson A., de Queiroz K., Losos J.B. 1999. Phylogenetic relationships and tempo of early diversification in Anolis lizards. Syst. Biol. 48:254–285.

James T.Y., Kauff F., Schoch C.L., Matheny P.B., Hofstetter V., Cox C.J., Celio G., Gueidan C., Fraker E., Miadlikowska J., Lumbsch H.T., Rauhut A., Reeb V., Arnold A.E., Amtoft A., Stajich J.E., Hosaka K., Sung G.H., Johnson D., O'Rourke B., Crockett M., Binder M., Curtis J.M., Slot J.C., Wang Z., Wilson A.W., Schussler A., Longcore J.E., O'Donnell K., Mozley-Standridge S., Porter D., Letcher P.M., Powell M.J., Taylor J.W., White M.M., Griffith G.W., Davies D.R., Humber R.A., Morton J.B., Sugiyama J., Rossman A.Y., Rogers J.D., Pfister D.H., Hewitt D., Hansen K., Hambleton S., Shoemaker R.A., Kohlmeyer J., Volkmann-Kohlmeyer B., Spotts R.A., Serdani M., Crous P.W., Hughes K.W., Matsuura K., Langer E., Langer G., Untereiner W.A., Lucking R., Budel B., Geiser D.M., Aptroot A., Diederich P., Schmitt I., Schultz M., Yahr R., Hibbett D.S., Lutzoni F., McLaughlin D.J., Spatafora J.W., Vilgalys R. 2006. Reconstructing the early evolution of Fungi using a six-gene phylogeny. Nature 443:818–822.

Janis C.M., Damuth J., Theodor J.M. 2000. Miocene ungulates and terrestrial primary productivity: where have all the browsers gone? Proc. Natl Acad. Sci. U.S.A. 97:7899–7904.

Joyce D.A., Lunt D.H., Bills R., Turner G.F., Katongo C., Duftner N., Sturmbauer C., Seehausen O. 2005. An extant cichlid fish radiation emerged in an extinct Pleistocene lake. Nature 435:90–95.

Keirle M.R., Hemmes D.E., Desjardin D.E. 2004. Agaricales of the Hawaiian Islands 8: Agaricaceae: Coprinus and Podaxis, Psathyrellaceae: Coprinellus, Coprinopsis and Parasola. Fung. Div. 15: 33–124.

Klak C., Reeves G., Hedderson T. 2004. Unmatched tempo of evolution in Southern African semi-desert ice plants. Nature 427:63–65.

Kozak K.H., Weisrock D.W., Larson A. 2006. Rapid lineage accumulation in a non-adaptive radiation: phylogenetic analysis of diversification rates in eastern North American woodland salamanders (Plethodontidae: Plethodon). Proc. Biol. Sci. 273:539–546.

Lanfear R., Ho S.Y., Love D., Bromham L. 2011. Mutation rate is linked to diversification in birds. Proc. Natl Acad. Sci. U.S.A. 107: 20423–20428.

Larsson E., Orstadius L. 2008. Fourteen coprophilous species of Psathyrella identified in the Nordic countries using morphology and nuclear rDNA sequence data. Mycol. Res. 112:1165–1185.
Lewis P.O., Holder M.T., Holsinger K.E. 2005. Polytomies and Bayesian phylogenetic inference. Syst. Biol. 54:241–253.
Lewis P.O., Holder M.T., Swofford D. 2010. Phycas 1.2.0 user manual. Distributed by the authors. Available from: http://hydrodictyon.eeb.uconn.edu/projects/phycas/index.php/Phycas_Home.
Lim H., Choi H.T. 2009. Enhanced expression of chitinase during the autolysis of mushroom in Coprinellus congregatus. J. Microbiol. 47:225–228.
Maddison P.W., Midford P.E., Otto S.P. 2007. Estimating a binary character's effect on diversification. Syst. Biol. 56:701–710
Marshall D.C. 2010. Cryptic failure of partitioned Bayesian phylogenetic analyses: lost in the land of long trees. Syst. Biol. 59:108–117.
Nagy G.L. 2006. Coprinus doverii sp. nov., a unique new species of subsection Setulosi from central and southern Europe. Mycotaxon 98:147–151.
Nagy G.L., Kocsubé S., Papp T., Vágvölgyi C. 2009. Phylogeny and character evolution of the coprinoid mushroom genus Parasola as inferred from LSU and ITS nrDNA sequence data. Persoonia 22: 28–37.
Nagy G.L., Walther G., Házi J., Vágvölgyi C., Papp T. 2011. Understanding the evolutionary processes of fungal fruiting bodies: correlated evolution and divergence times in the Psathyrellaceae. Syst. Biol. 60(3):303–317.
Nagy L.G., Urban A., Orstadius L., Papp T., Larsson E., Vagvolgyi C. 2010. The evolution of autodigestion in the mushroom family Psathyrellaceae (Agaricales) inferred from Maximum Likelihood and Bayesian methods. Mol. Phylogenet. Evol. 57: 1037–1048.
Nee S. 2001. Inferring speciation rates from phylogenies. Evolution 55:661–668.
Organ C.L., Janes D.E., Meade A., Pagel M. 2009. Genotypic sex determination enabled adaptive radiations of extinct marine reptiles. Nature 461:389–392.
Örstadius L. 2008. Psathyrella. In: Knudsen H., Vesterholt J., editors. Funga Nordica. Copenhagen (Denmark): NordSvamp. p. 586–623.
Padamsee M., Matheny P.B., Dentinger B.T., McLaughlin D.J. 2008. The mushroom family Psathyrellaceae: evidence for large-scale polyphyly of the genus Psathyrella. Mol. Phylogenet. Evol. 46: 415–429.
Pagel M. 1994. Detecting correlated evolution on phylogenies: a general method for the comparative analysis of discrete characters. Proc. Biol. Sci. 255:37–45.
Pagel M. 1997. Inferring evolutionary processes from phylogenies. Zool. Scripta. 26:331–348.
Pagel M. 1999a. Inferring the historical patterns of biological evolution. Nature 401:877–884.
Pagel M. 1999b. The maximum likelihood approach to reconstructing ancestral character states of discrete characters on phylogenies. Syst. Biol. 48:612–622.
Pagel M., Meade A. 2005. Mixture models in phylogenetic inference. In: Gascuel O., editor. Mathematics of evolution and phylogeny. Oxford: Oxford University Press. p. 121–142.
Pagel M., Meade A. 2007a. BayesPhylogenies 1.0. Distributed by the author. Available from: http://www.evolution.rdg.ac.uk.
Pagel M., Meade A. 2007b. Bayestraits 1.0. Distributed by the author. Available from: http://www.evolution.rdg.ac.uk.
Pagel M., Venditti C., Meade A. 2006. Large punctuational contribution of speciation to evolutionary divergence at the molecular level. Science 314:119–121.
Paradis E., Claude J., Strimmer K. 2004. APE: analyses of phylogenetics and evolution in R language. Bioinformatics 20:289–290.
Posada D. 2008. jModelTest: phylogenetic model averaging. Mol. Biol. Evol. 25:1253–1256.
Purvis A. 2004. Evolution: how do characters evolve? Nature 432:165.
Rabosky D.L. 2006. LASER: a maximum likelihood toolkit for detecting temporal shifts in diversification rates from molecular phylogenies. Evol. Bioinform. Online 2:273–276.
Rabosky D.L., Lovette I.J. 2008. Density-dependent diversification in North American wood warblers. Proc. Biol. Sci. 275:2363–2671.
Rambaut A., Drummond A. 2008a. BEAST. Distributed by the author. Available from: http://beast.bio.ed.ac.uk/.
Rambaut A., Drummond A. 2008b. Tracer v. 1.4.1. Distributedby the authors. Available from: http://beast.bio.ed.ac.uk/.
Rannala B. 2002. Identifiability of parameters in MCMC Bayesian inference of phylogeny. Syst. Biol. 51:754–760.
Reijnders A.F.M. 1979. Developmental anatomy of Coprinus. Persoonia 10:383–424.
Richardson J.E., Pennington R.T., Pennington T.D., Hollingsworth P.M. 2001. Rapid diversification of a species-rich genus of neotropical rain forest trees. Science 293:2242–2245.
Ricklefs R.E. 2004. Cladogenesis and morphological diversification in passerine birds. Nature 430:338–341.
Roshan U., Livesay D.R. 2006. Probalign: multiple sequence alignment using partition function posterior probabilities. Bioinformatics 22:2715–2721.
Rundell R.J., Price T.D. 2009. Adaptive radiation, nonadaptive radiation, ecological speciation and nonecological speciation. Trends Ecol. Evol. 24:394–399.
Sanderson M.J., Donoghue M.J. 1994. Shifts in diversification rate with the origin of angiosperms. Science 264:1590–1593.
Schluter D. 2000. The ecology of adaptive radiations. Oxford: Oxford University Press.
Shimodaira H. 2002. An approximately unbiased test of phylogenetic tree selection. Syst. Biol. 51:492–508.
Shimodaira H., Hasewaga M. 2001. CONSEL: for assessing the confidence of phylogenetic tree selection. Bioinformatics 17:1246–1247.
Skinner A. 2010. Rate heterogeneity, ancestral character state reconstruction and the evolution of limb morphology in lerista (Scincidae, Squamata). Syst. Biol. 59:723–740.
Stamatakis A. 2006. RAxML-VI-HPC: maximum likelihood-based phylogenetic analyses with thousands of taxa and mixed models. Bioinformatics 22:2688–2690.
Struck T.H., Paul C., Hill N., Hartmann S., Hosel C., Kube M., Lieb B., Meyer A., Tiedemann R., Purschke G., Bleidorn C. 2011. Phylogenomic analyses unravel annelid evolution. Nature 471:95–98.
Thompson J.D., Gibson T.J., Higgins D.G. 2002. Multiple sequence alignment using ClustalW and ClustalX. Curr. Protoc. Bioinformatics Chapter 2: Unit 2 3. Available from: http://onlinelibrary.wiley.com/doi/10.1002/0471250953.bi0203s00/abstract.
Uljé C.B. 2005. Coprinus. In: Noordeloos M.E., Kuyper T.W., Vellinga E.C., editors. Flora Agaricina Neerlandica. Volume 6. Boca Raton (Fl): CRC press. p. 22–109.
Uljé C.B., Bas C. 1991. Studies in Coprinus-II. Subsection Setulosi of section Pseudocoprinus. Persoonia 14:275–339.
Valente L.M., Savolainen V., Vargas P. 2010. Unparalleled rates of species diversification in Europe. Proc. Biol. Sci. 277:1489–1496.
Vasutova M., Antonin V., Urban A. 2008. Phylogenetic studies in Psathyrella focusing on sections Pennatae and Spadiceae—new evidence for the paraphyly of the genus. Mycol. Res. 112:1153–1164.
Verheyen E., Salzburger W., Snoeks J., Meyer A. 2003. Origin of the superflock of cichlid fishes from Lake Victoria, East Africa. Science 300:325–329.
Walther G., Garnica S., Weiss M. 2005. The systematic relevance of conidiogenesis modes in the gilled Agaricales. Mycol. Res. 109: 525–544.
Wilgenbusch, J.C., Warren D.L., Swofford D.L. 2004. AWTY: a system for graphical exploration of MCMC convergence in Bayesian phylogenetic inference. Available from: http://ceb.csit.fsu.edu/awty.